Pure MnO_2, Ni/MnO_2, Ni/MnO_2@PVA and Ni/MnO_2@PVP polymetrix nanocomposites for energy storage device

M. Sivakumar [a*], P. Kanakarajan [a], V. Jeevanantham [b]
[a] *Department of Mechanical Engineering, KSR Institute for Engineering and Technology, Tiruchengode – 637215, India*
[b] *Department of Chemistry, Vivekanandha College of Arts and Sciences for Women(Autonomous), Tiruchengode-637205, India*

In the last few years, there have been a great deal of discoveries and research made that has contributed to the development of Metal-based polymer nanocomposites. Electromagnetic shielding, energy storage devices, fuel cells, membranes, sensors, and actuators are just some of the many intriguing uses for Metal-based materials and their composites. Experiments using cyclic voltammetry investigated the super capacitive qualities of MnO_2 nanoparticles, MnO_2 nanoparticles that had been doped with nickel, and MnO_2 nanoparticles that had been combined with Poly-vinyl-alcohol (PVA) and Poly-vinyl-Pyrolidone (PVP). A method known as hydrothermal synthesis was used in the production of both the polymer nanocomposites and the nanoparticles. Analyses using Fourier transform infrared spectroscopy (FTIR) and X-ray diffraction (XRD) revealed the structural changes that occurred as a result of the interaction between MnO_2/Ni and the PVA/PVP mix matrix. Examining the surface morphology of synthesized nanocomposite films was carried out with the assistance of scanning electron microscopy (SEM). Through the use of cyclic voltammetry, it was discovered that the values of capacitance for MnO_2, nickel doped MnO_2, and nickel doped Polymer capped MnO_2 nanoparticles, respectively, were 164F/g, 293F/g, 304F/g, and 471.9F/g. In contrast to nickel doped MnO_2 nanoparticles that were assisted by PVP, nickel doped MnO_2 nanoparticles that were assisted by PVA were shown to be a more effective super capacitor.

(Received November 10, 2023; Accepted April 4, 2024)

Keywords: MnO_2, Nanocomposites, Capacitance, Polymetrix

1. Introduction

Alternatives to chemicals obtained from petroleum need a basis of carbon fragments, however renewable sources such as solar and wind energy have the potential to satisfy the world's demand for energy. It is required to develop a means to store the energy that is generated by renewable energy sources before it can be utilized. This is due to the fact that renewable energy sources do not exist in a vacuum. The evolution of electronic devices that are smaller and more portable has placed a renewed emphasis on the research and development of energy storage systems that are more efficient. Over the course of the last two decades, storage capacity have expanded considerably, but at the same time, the sizes of portable tools and gadgets such as smartphones, laptops, and smart health devices have decreased noticeably over this same time period. The energy markets for these instruments are, understandably, fairly saturated, and as a result, this has prompted a huge rise in the amount of research that is directed at high-performance applications. One of the most important types of research in the field of energy in recent years is the use of supercapacitors in batteries. The flat charge curve of the supercapacitor supports the device's high energy density. The goal of ongoing research is to create a new type of supercapacitor [1]. The size, shape and crystal structure of MnO_2 nanoparticles have a direct impact on their electrochemical performance [2, 3], and MnO_2 is one of the supercapacitor materials due to its low toxicity and cheap price. Nanoparticles containing MnO_2 are now recognized as useful candidates for media [4]. Photocatalysts, electrodes for rechargeable batteries,

* Corresponding author: sivakumarmmech@yahoo.com
https://doi.org/10.15251/JOR.2024.202.201

electrocatalysts for fuel cells, and supercapacitors are some of the uses of MnO_2 nanoparticles in energy storage [5]. Addition of nickel to MnO_2 nanoparticles leads to an increase in the specific capacitance value [6, 7]. The structure of polymers such as polyvinyl alcohol (PVA) can be modified by doping with nanoparticles. In particular, mixing transition metal salts with nanoparticles is a good way to achieve this goal and leads to new materials with improved microstructural, optical, electrical and thermal properties [8]. The purpose of this study was to investigate the structure, surface morphology, and optical features of very flexible porous MnO2, Ni/MnO2 nanoparticles, Ni/MnO2/PVA, and Ni/MnO2/PVP nanocomposites films for electrochemical (supercapacitor electrodes) applications.

2. Experimental procedure

2.1. Synthesis of MnO_2, Ni/MnO_2nanoparticles, Ni/MnO_2/PVA and Ni/MnO_2/PVP nanocomposites

In most cases, the production of MnO_2 nanoparticles involves hydrothermally treating 0.17 grams of $MnCl_2$ that has been dissolved in 50 milliliters of ethanol with 0.10 grams of $KMnO_4$ at a temperature of 73 degrees Celsius. The hydrothermal synthesis procedure was used to produce Ni/MnO_2 nanoparticles in the same way as $NiCl_2$ was produced. After adding the $KMnO_4$, the pink tint changes to a brown color, and after waiting for six hours, a brown precipitate develops at the bottom of the round-bottom flask. After a period of reflection lasting six hours, the particles that have formed are filtered, and any leftover contaminants are removed by washing them with ethanol (three times). Following a period of 24 hours spent within the micro-oven, the nanoparticles were taken out of the oven and given time to dry. Ni/MnO_2/PVA and Ni/MnO_2/PVP nanocomposites were produced by following the same procedure and adding 0.1 g of poly vinyl alcohol (PVA) and 0.15 g of poly vinyl pyrolidine (PVP) to the reaction mixture, respectively.

3. Results and discussions

3.1. XRD analysis of MnO_2, Ni/MnO_2 NPs and Ni/MnO_2/PVA, Ni/MnO2/PVP NCs

The XRD research makes it easier to conduct an analysis of the structural properties of the material. A 1.5460A° X-ray diffractometer was used to examine the powder X-ray diffraction patterns of MnO_2, Ni/MnO_2 nanoparticles, Ni/MnO_2/PVA and Ni/MnO_2/PVP nanocomposites. At room temperature, MnO_2 and Ni/MnO_2 XRD patterns were photographed with the assistance of PVA and PVP. With the help of the XRD analysis, determine the usual crystalline size of the samples. The aircraft (111), (112), and (201) had the most prominent peaks, whereas plane (101) displayed the least obvious peaks. The crystalline diameters of the nanocomposite sizes of MnO_2, Ni/MnO_2, Ni/MnO_2/PVA, and Ni/MnO_2/PVP were found to be, 56.25, 48.73 nm, 43 nm, and 41.72 nm, respectively.

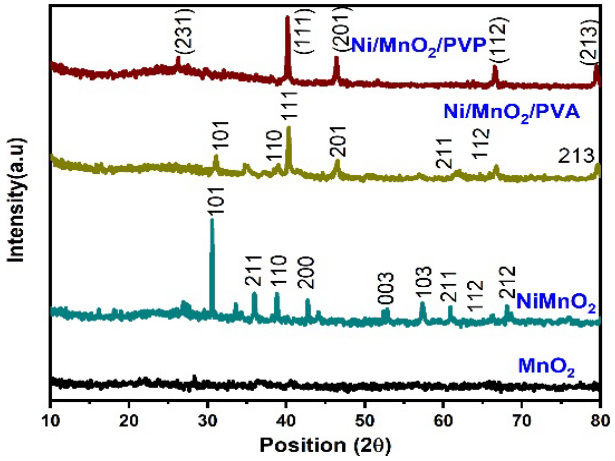

Fig. 1. XRD patterns of MnO_2, Ni/MnO_2 NPs and Ni/MnO_2/PVA and Ni/MnO_2/PVP NCs.

The calculation of average crystallite size was performed with the Debye-Scherrer formula.

$$D = 0.9\,\lambda / \beta\, Cos\theta \quad (1)$$

D here stands for the typical domain size of crystallites in nanometers (nm), while λ stands for the wavelength of X-rays, which is around 1.5406 x 10^{-10} m. The FWHM of is being addressed here; that is β, its full width at half its maximum in radians. The diffraction angle is denoted by the symbol and is θ expressed in degrees. The numerical value of the symbol K is -0.94. X-ray diffraction (XRD) examination was used to assess the crystalline size and d-spacing of MnO_2, Ni/MnO_2 nanoparticles, and Ni/MnO_2/PVA, Ni/MnO_2/PVP nanocomposites. The results of this research are shown in Table 1, along with any relevant information.

Table 1. Crystalline size and d-spacing of prepared NPs and NCs by XRD.

S.no	Samples	Crystalline size (nm)	D-spacing (%)
1	Mn-O_2	56.25	-
2	Ni/Mn-O_2	48.73	3.12287
3	Ni/MnO_2/PV-A	43	2.33651
4	Ni/MnO_2/PV-P	41.72	2.34686

3.2. Morphological study of MnO_2, Ni/MnO_2 nanoparticles, Ni/MnO_2/PVA, Ni/MnO_2/PVP nanocomposites by SEM

Images obtained by scanning electron microscopy (SEM) of MnO_2, Ni/MnO_2 nanoparticles, Ni/MnO_2/PVA, and Ni/MnO_2/PVP nanocomposites are shown in Figure 2. The image obtained by scanning electron microscopy (SEM) showed that there were nanoparticles present, each of which had a crystalline structure. The use of imaging methods with a high magnification indicates that the small crystals have a spherical shape as they undergo development into bigger crystal formations. This was discovered via the use of imaging techniques.

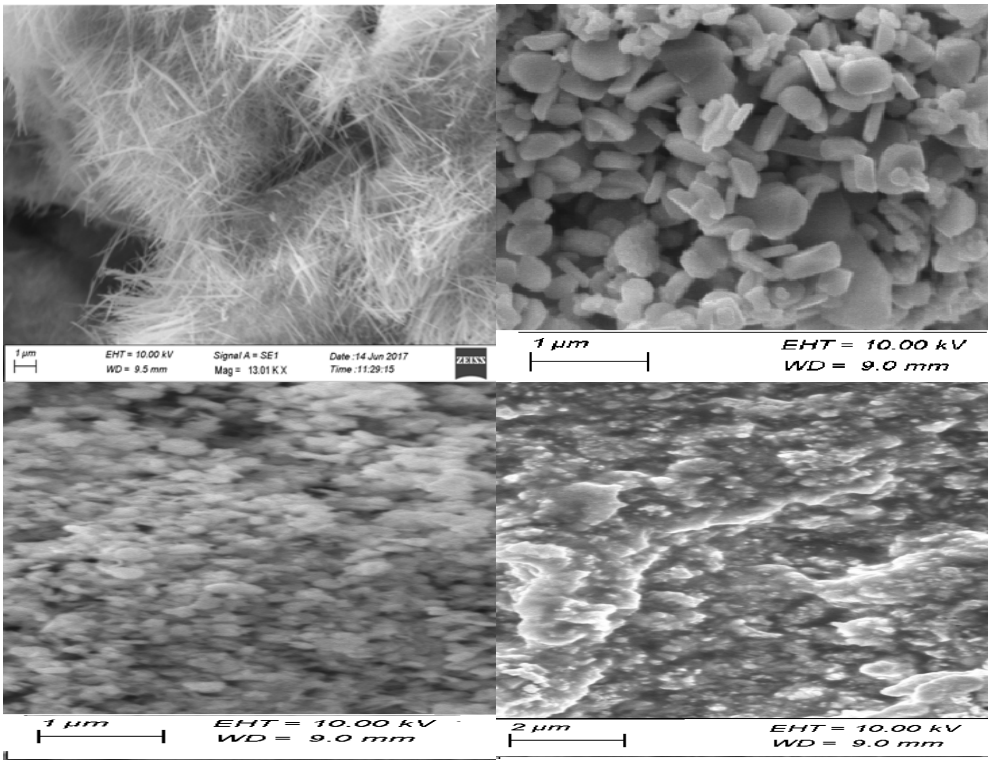

Fig. 2. SEM analysis of MnO_2, Ni/MnO_2 NPs and Ni/MnO_2/PVA and Ni/MnO_2/PVP NCs.

3.3. UV-Visible absorption spectra of MnO_2, Ni/MnO_2 nanoparticles and Ni/MnO_2/PVA, Ni/MnO_2/PVP nanocomposites

The band gap energy is shown to decrease with increasing particle size, according to the findings of studies on the absorption of UV and visible light by the nanoparticles and nanocomposite as they were synthesized. The energy gaps for different nanocomposites made of manganese dioxide and nickel monoxide range from 3.67 eV to 3.52 eV to 3.34 eV to 3.13 eV. In the absorption spectra of MnO_2, Ni/MnO_2, Ni/MnO_2/PVA, and Ni/MnO_2/PVP, respectively, there were discernible excitonic peaks located at 201, 219, 237, and 262nm nm.

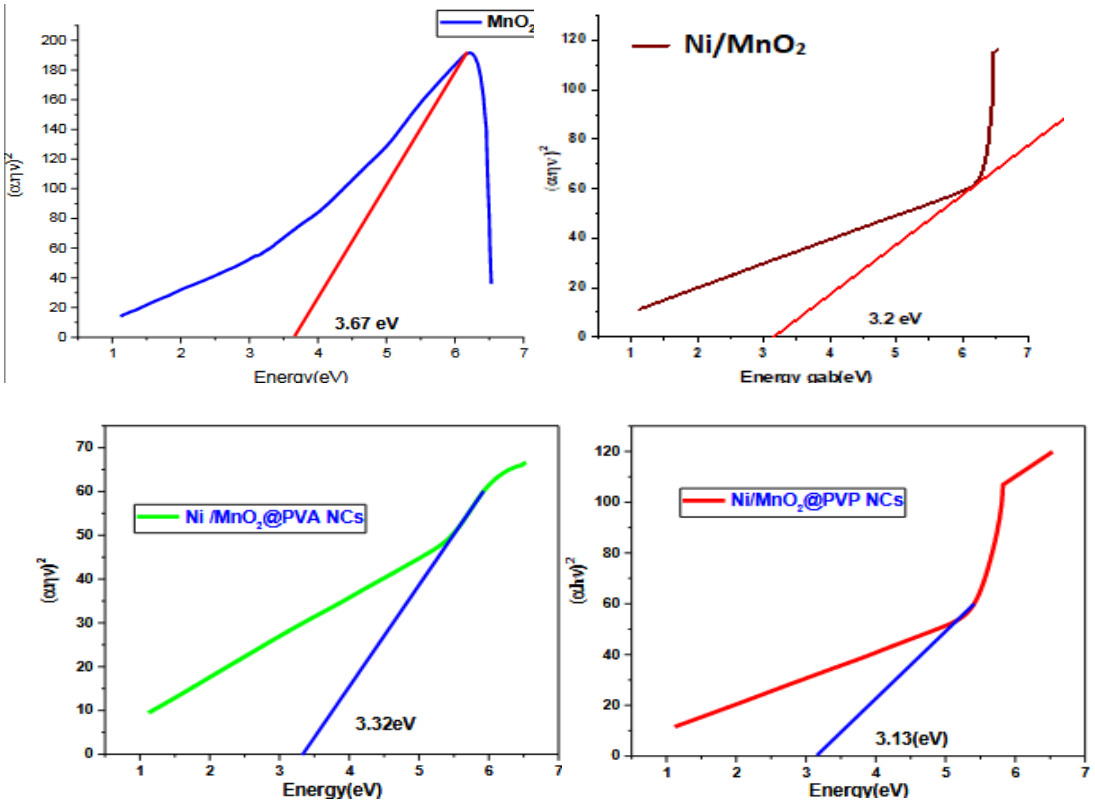

Fig. 3. UV-Visible-spectra of MnO_2, Ni/MnO_2 NPs and Ni/MnO_2/PVA and Ni/MnO_2/PVP NCs.

3.4. Functional group analysis of MnO_2, Ni/MnO_2 nanoparticles and Ni/MnO_2/PVA, Ni/MnO_2/PVP nanocomposites by FTIR

The FTIR spectrum was utilized to examine the structural information of the functional groups that make up synthesized nanoparticles and nanocomposites, as well as to identify the composition of synthesized nanoparticles and nanocomposites. The bending and stretching vibrations of C=O are the cause of the characteristics that peak between 1540 and 3400 cm^{-1}. An absorption peak that ranges from around 760 cm^{-1} to 508 cm^{-1} is distinguishes the Ni and Mn-O bands.

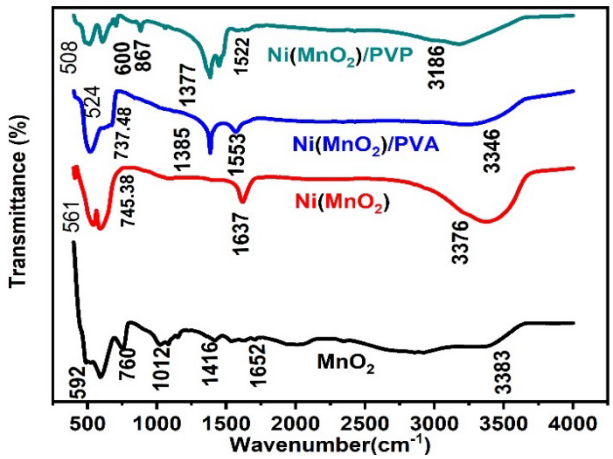

Fig. 4. FT-IR spectra of MnO_2, Ni/MnO_2 NPs and Ni/MnO_2/PVA and Ni/MnO_2/PVP NCs.

3.5. Measurement of specific capacitance value for MnO_2, Ni/MnO_2, Ni/MnO_2/PVA and Ni/MnO_2/PVP nanocomposites by cyclic voltammetry (CV) study

The outcomes of cyclic voltammetric tests performed on pure MnO_2, Nickel doped MnO_2 nanoparticles, Nickel doped MnO_2 assisted by PVA, and PVP nanocomposites are shown in Fig.4, which was generated at a scan rate of 2mV/s. According to the results of the cyclic voltammetry test, the capacitance value is as follows:

$$Specific\ capacitance\ =\ Area/2\ x\ scan\ rate\ x\ potential\ window\ x\ mass\ of\ the\ element \quad (2)$$

The values of capacitance were found to be as follows: 164 F/g for MnO_2, 293 F/g For Ni/MnO_2 nanoparticles; 304 F/g for Ni/MnO_2/PVA; 47.19 F/g for Ni/MnO_2/PVP nanocomposites. Because doping a polymer may change its molecular structure, our voltammetric results reveal that the redox potential behaviour of these nanocomposites was lowered with increased doping and aid from polymers. This was the case despite the fact that the nanocomposites included polymers. Polymers that have transition metals and nanoparticles incorporated into them undergo a change in their physical features [9-11]. The addition of PVA, which is a water-soluble polymer that has a hydrogen connection between the hydroxyl group and water molecules [12, 13], is the reason why the Ni/MnO_2/PVA composite has such a high specific capacitance value, as was shown before. PVA-based composites were shown to possess polar polymeric properties [16-20].

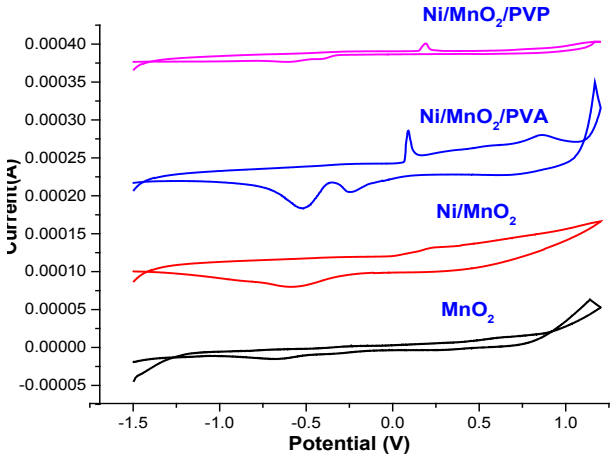

Fig. 5. Cyclic voltagram of MnO_2, Ni/MnO_2 NPs and Ni/MnO_2/PVA and Ni/MnO_2/PVP NCs.

4. Conclusions

A hydrothermal technique was used to synthesize nanoparticles of pure MnO_2, Ni-doped MnO_2, Ni/MnO_2/PVA, and Ni/MnO_2/PVP respectively. Both the crystalline size and the particle size of the as-synthesized particles were found to be within the range of 100 nm when analyzed by XRD and SEM respectively. In order to identify the various functional classes of nanocomposites, FTIR spectroscopy was carried out. Using CV, the specific capacitance of as-synthesized nanoparticles and nanocomposites was analyzed, and the results showed that the Ni/MnO_2/PVA nanocomposites had the greatest value. This is due to the polar nature of the PVA polymer, as well as the fact that the hydroxyl group on the chain interacts with water molecules in order to boost the specific capacitance.

References

[1] Ming Huang, Fei Li, FanDong, Yuxin Zhang, Li Li Zhang, Journal of Material Chemistry A

[2] Jian-Gand Wang, Bingquing, Engineering of MnO2 based nanocomposites for high performance super capacitor, Elsvier

[3] Pavinda Kanha, Pimial Ssaengkwam Sawang. Inorganic and Nanometal chemistry vol47-2017 isuue 8; https://doi.org/10.1080/24701556.2017.1284100

[4] S. R. Srither, A. Karthick, D. Murugesan, S. Arun Metha, M. Selvam, V. Rajendran.. Frontiers in Nanoscience and Nanotechnology

[5] Jing-Juan Xu. Hong-Yuan, Science Direct vol- 6 isuue 11 ,Nov-2004; https://doi.org/10.1016/j.elecom.2004.09.015

[6] R. Poonguhali, R. Gobi, N. Shanmugam, G. Viruthagiri, IJARTET

[7] Landan, W. J. Basirun, S. N. Xaxi, F. A. Rahaman, 2017 Material Chemistry and Physics 192361-373

[8] Tuncay Tunc, Habibe Uslu, Semettin Altindal, Polymers 2011,vol.12 No- 7; https://doi.org/10.1007/s12221-011-0886-6

[9] H. M. Zidan, Journals of Polmers Sci -88, 1115(2003); https://doi.org/10.1002/app.12123

[10] R. F. Bhajatri, V. Ravindrachry, A. Hanisha, V. Grasta, S. P. Nayaland, B. Poojang, Polymers, 47, 3591(2006)

[11] R. F. Bhajatri, V. Ravindrachry, A. Harisha, C. Ranganathaiah, G. N. Kumaraswamy, Applied Phy. A 87, 797(2007); https://doi.org/10.1007/s00339-007-3923-y

[12] Bhuvaneshwari, S. Satheeskumar, S. Jeevanantham Velayutham. Rahman, B. S. *Rasayan J. Chem*, 2021,*14*, 1581-1586. http://doi.org/10.31788/ RJC.2021.1436022

[13] Gopinatha, P. Suresh, P. & Jeevanantham, V. Journal of Ovonic Research, (2023). 19(1). https://doi.org/10.15251/JOR.2023.191.23

[14] Jeevanantham, V. Tamilselvi, D. Rathidevi, K. Bavaji, S. R. & Neelakandan, P. *Biomass Conversion and Biorefinery*, 2023, 1-10; https://doi.org/10.1007/s13399-023-04179-9

[15] N. R. Stradiotto, K. E. Toghill, L. Xiao, A. Moshar, R. G. Comptonb, Electroanalysis, 2009, 21, 2627-2633; https://doi.org/10.1002/elan.200900325

[16] Danaee, M. Jafarian, A. Mirzapoor, F. Gobal, M. G. Mahjani, Electrochim. Acta, 2010, 55, 2093-2100; https://doi.org/10.1016/j.electacta.2009.11.039

[17] V. L. Oliveira, C. Morais, K. Servat, T. W. Napporn, G. Tremiliosi-Filho, K. B. Kokoh, Electrochim. Acta, 2014, 117, 255-262; https://doi.org/10.1016/j.electacta.2013.11.127

[18]. N. Yu, L. Gao, Electrochem Commun. 11 (2009)220; https://doi.org/10.1016/j.elecom.2008.11.013

[19]. S Arul, T Senthilnathan, V Jeevanantham, KV Satheesh Kumar, Archives of Metallurgy and Materials, 2021, 6(4), 1141-1148. https://doi.org/10.24425/amm.2021.136434

[20] Jeevanantham, V. Tamilselvi, D. Rathidevi, K. & Bavaji, S. R. *Journal of Materials Research*, 2023, *38*(7), 1909-1918. https://doi.org/10.1557/s43578-023-00965-3